A 10.6mm^3 Fully-Integrated, Wireless Sensor Node with 8GHz UWB Transmitter

Hyeongseok Kim, Gyouho Kim, Yoonmyung Lee, Zhiyoong Foo, Dennis Sylvester, David Blaauw, David Wentzloff
University of Michigan, Ann Arbor, MI, E-mail: hskims@umich.edu

Abstract

This paper presents a complete, autonomous, wireless temperature sensor, fully encapsulated in a 10.6mm^3 volume. The sensor includes solar energy harvesting with an integrated 2 μAh battery, optical receiver for programming, microcontroller and memory, 8GHz UWB transmitter, and miniaturized custom antennas with a wireless range of 7 meters. Full, stand-alone operation was demonstrated for the first time for a system of this size and functionality.

Introduction

Recently there has been increased demand for a millimeter-scale wireless sensor node for applications such as biomedical devices, defense and surveillance. This form-factor is driven by a desire to be vanishingly small, injectable through a needle, or implantable through a minimally-invasive surgical procedure. Wireless communication is a necessity, but at the millimeter-scale the antenna size and power consumption of the electronics has limited communication range to only a few centimeters [1-2]. This work introduces a fully integrated wireless sensor that enables meter-range communication with a base station using two custom antennas, a monopole and dipole, co-designed with a UWB transmitter to optimize radiated power. The complete sensor node is energy autonomous, sustainable with a 2mm sized, 2 μAh battery and an integrate solar cell.

Proposed System

The overall system block diagram is shown in Fig. 1. The circuits are implemented in a heterogeneous 8-layer stack of thinned die, which communicate via MBus, a fully digital interconnect bus scheme suitable for energy-constrained sensing systems [3]. The processor layer contains an ARM Cortex-M0 microcontroller along with a power management unit which down-converts the battery voltage to generate 1.2 V and 0.6 V power domains distributed across the stack [2]. The battery is a 2 μAhr solid state thin film Li rechargeable battery supplied by Cymbet that operates between 3.6-4.2 V. A 3 kB SRAM serves as instruction and data memory. A sensor layer contains the temperature sensor and a 13-bit CDC that can be used for optional pressure measurements. A self-starting energy harvester [4] can up-convert the solar cell output with a configurable conversion ratio to charge the battery. The radio layer contains an UWB transmitter with a tunable output frequency from 8 to 11GHz and a current limiter to protect the battery from over-current when the radio is on [2]. Finally, the dies are stacked on a glass substrate including a printed, 8GHz wideband antenna co-designed with the UWB transmitter. The entire system including the glass substrate is encapsulated with epoxy for physical protection (Fig. 2), which raises unique challenges for the initial battery charging and system boot up of the fully encapsulated system.

Antennas and UWB transmitter

The antenna and UWB transmitter are co-designed in order to miniaturize the antenna size, and eliminate the need for an off-chip matching network. The primary goal is to maximize the radiated power by reducing the mismatch between the transmitter and antenna, and minimizing the impact of the die stack which is placed in close proximity to the radiating element. When the separation is too close, the antenna gain reduces significantly due to the reflection from the IC layers and the discontinuity in effective dielectric constants of the materials. To simultaneously minimize the antenna dimensions and electrical mismatch, the output of the transmitter and the input of the antenna both are matched to 10 Ohms without using off-chip matching network.

This paper demonstrates the sensor node operating with two antennas, a monopole and dipole. Both antennas are fabricated on a glass substrate with lower substrate loss than silicon, to achieve higher antenna efficiency. The dimensions of the antennas are 0.05λo x 0.11λo which includes the ground plane. A monopole has an advantage that could save the physical antenna area by using its ground plane as reflector. However, when the monopole is considered as small antenna that is much smaller than the wavelength, the antenna gain is not determined from antenna element itself, but by its ground plane and environment, which in this case also includes the sensor node die stack. A dipole antenna with a merchant balun isolates these environmental and ground plane effects. (Fig. 3) The lossy epoxy used for encapsulation degrades the antenna gain and shifts the resonance frequency, which leads to a shorter communication distance compared to free-space. The antenna design and results are summarized in Fig. 4.

Fig. 5 shows a test setup between the die-stacked sensor node and a base station, and the equivalent isotopically radiated power (EIRP) at the transmitter as a function of center frequency. This EIRP can be used to determine the base-station sensitivity for a target distance (Fig. 6). For the distance test, the received signal was amplified and down-converted to an IF (150MHz) before being observed on an oscilloscope to verify functionality. The base-station has 52.8dB gain and 10dB noise figure at IF and -99dBm sensitivity including the receiver antenna gain. The measured communication range for the dipole was 7 meters with a peak SNR of 10dB. (Fig. 7)

Assembly and Sequencing

With a millimeter-scale form factor, wired physical connections to the unit are infeasible from a yield and usability perspective and the entire unit is encased in epoxy. In this paper, we present the first fully wireless startup of a system of this size, including battery charging. The battery is initially uncharged after fabrication, and must remain so during the assembly process to endure the high temperature epoxy curing. With exposure to light of ~200 lux (dim indoor light) the harvester is able to self-start and commence battery charging, with a minimum solar cell output voltage of 140mV and power of 1.6nW. Fig. 8 shows a measured battery charging curve when energy is harvested under 25kLux light which requires 15.5 hours to fully charge the integrated battery. As the charged battery voltage rises beyond 3.6V, the system automatically initiates a boot sequence. Initially, the PMU raises the 1.2V supply and holds the 0.6V supply to ground. This state is detected by reset detectors in each layer to generate clean reset signals for critical blocks such as the configuration registers. Subsequently, the 0.6V supply is raised, and the system enters a sleep mode, in which the core is still power-gated and the SRAM has no content. The reset values of configuration registers ensure that the circuit components are either power-gated or in an ultra-low power state.

Once the battery is fully charged, the system is programmed via optical communication to load the SRAM with a program [5]. The front-end photodiodes of the optical receiver are placed in the SOLAR layer located at the top of the stack for light exposure through clear epoxy, such that the rest of the stack can be encapsulated with black epoxy to minimize light-induced leakage current in the ICs. Optical communication can also directly change the configuration register settings or send interrupts. Once the SRAM is loaded, system operation commences, switching between sleep and active modes and communicating with blocks in different layers via MBus. Fig. 8 shows the current consumption of the sensor system programmed to transmit data once every 5 seconds. In sleep mode, it consumes 2nA and in active mode current jumps to ~9μA for 700ms. The initial current peak upon wake up is due to the charging of decoupling caps on power-gated supplies and no overcurrent is observed during radio transmission due to the current limiter in the Radio layer.

Conclusion

Table 1 summarizes the measured performances of the wireless sensor node with comparison to the state of the art. This sensor node has total volume of 10.6mm^3, while achieving microwatt power and

meter-range communication. A figure of merit of communication distance per volume is introduced, which highlights how this work compares to state of the art. The die micrograph of the stack is shown in Fig. 9.

Acknowledgements

This work was supported by the National Science Foundation under Grant No. CNS-1111541. The authors thank Cymbet, RTI, Advotech for assembly/encapsulation support.

References

[1] J Brown, et al., ISSCC, pp. 442-443, Feb 2013
[2] Y Lee, et al., ISSCC, pp. 402-404, Feb 2012
[3] Y.-S. Kuo, et al., CICC, pp. 1-4, Sep 2014
[4] W. Jung, et al., ISSCC, pp. 398-399, Feb 2014
[5] G Kim, et al., VLSI, pp. 141-142, Jun 2014
[6] G Ono, et al., VLSI, pp. 90-91, Jun 2007
[7] M Danesh, et al., MTT, pp. 3546-3555, Dec 2011

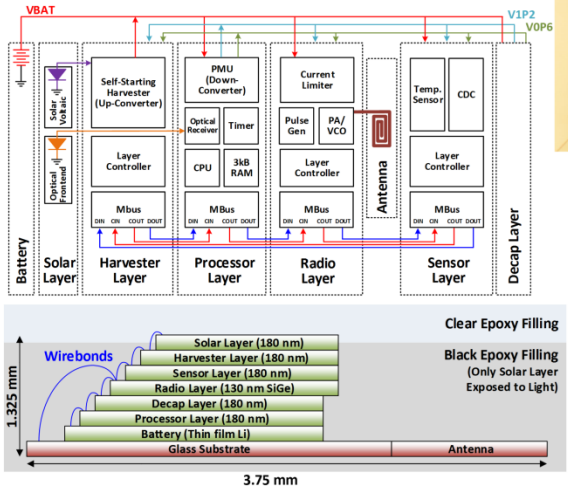

Figure 1. Overall system block diagram (top) and conceptual diagram (bottom).

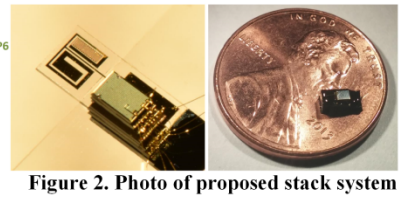

Figure 2. Photo of proposed stack system and encapsulated stack

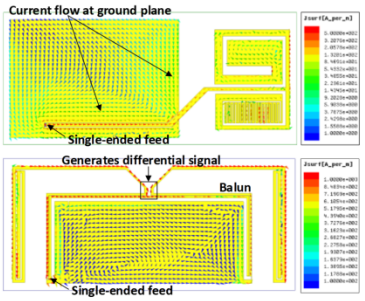

Figure 3. Suface current distribution of monopole and dipole

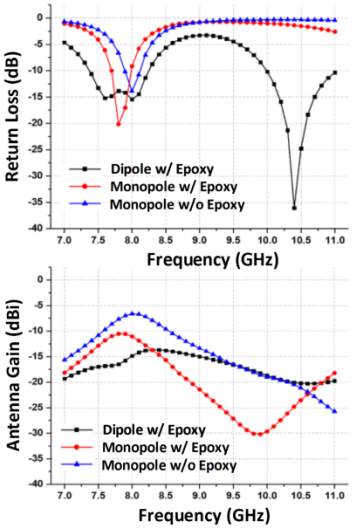

Figure 4. Return loss (S11) and antenna gain variation

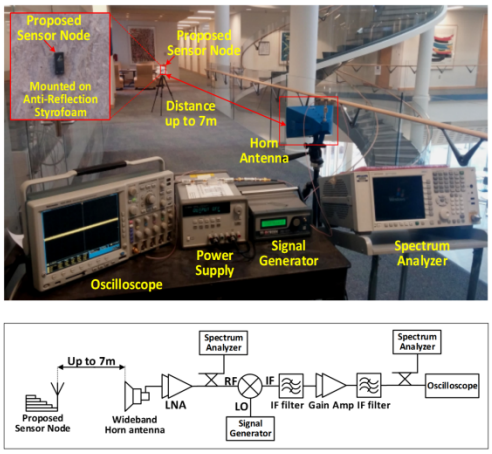

Figure 5. Measurement setup and block diagram of a receiver

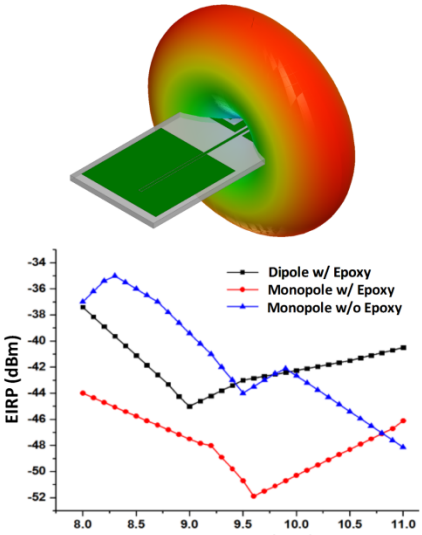

Figure 6. 3D radiation pattern and measured EIRP by sweeping VCO

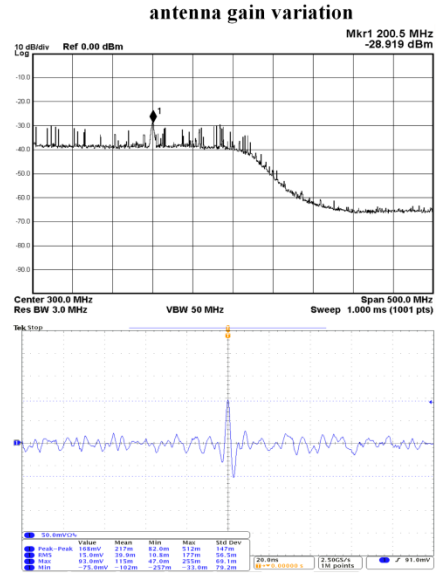

Figure 7. Received signal at SA (top) and a received pulse at OSC (bottom)

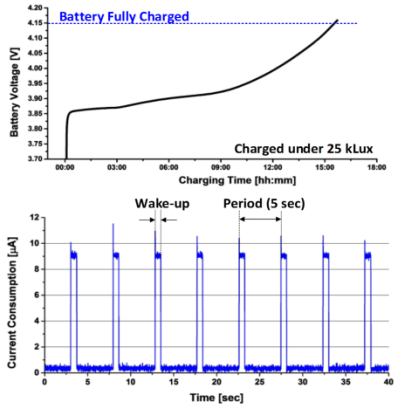

Figure 8. Battery charging characteristic under 25kLux light and current consumption in sleep and active mode

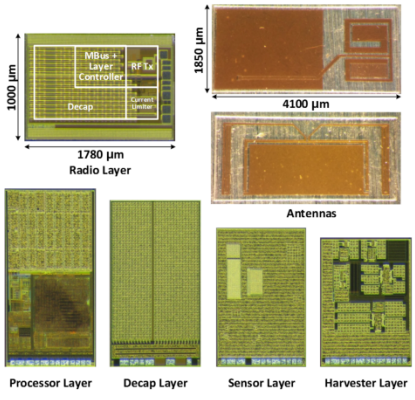

Figure 9. Die photos of Processor, Decap, Sensor, Harvester, Solar, Radio and Antenna layers

		This work			VLSI 2014 [5]	VLSI 2007 [6]	MTT 2011 [7]
		Dipole w/ Epoxy	Monopole w/ Epoxy	Monopole w/o Epoxy			
Dimension [mm³]		1.85 x 4.1 x 1.4			2 x 4 x 4	10 x 10 x 10	40 x 22 x 1.1
Power	Active	36 µW			40 µW	36 mW	5.4 mW
	Standby	8 nW			15 nW	1.8 µF	7.2 µW
Distance		7.0 m	3.8 m	13.4 m	15 mm	10 m (10.7 Mbps)	60 m
Distance/Volume [Normalized]		1	0.54	1.91	0.0007	0.015	0.094
Wireless		8.0 GHz			Optical Receiver RF Transmitter	Original UWB	3.6-4.1 GHz
Battery Capacity		2 µAh Thin-Film			5.7 µAh Thin-Film	150 mAh	-

Table 1. Measurement summary and performance comparison.